The Scientific Temper (2023) Vol. 14 (3): 696-702

E-ISSN: 2231-6396, ISSN: 0976-8653

Doi: 10.58414/SCIENTIFICTEMPER.2023.14.3.19

https://scientifictemper.com/

RESEARCH ARTICLE

Automatic liver tumor segmentation from CT images using random forest algorithm

N. Sasirekha[1*], R. Anitha[2], Vanathi T[3] and Umarani Balakrishnan[4]

Abstract

Automatic liver segmentation is challenging, and the tumor segmenting process adds more complexity. Based on the grey levels and shape, separating the liver and tumor from abdominal CT images is critical. In our paper suggests a more effective approach by using Gabor features (GF) to segment liver tumors from CT images and three alternative neural network algorithms to address these problems: RF, CNN and ANN. This thesis uses the same collection of classifiers and GF to first segment a variety of Gabor liver images. The organ (liver) is then extracted from an abdominal CT image using liver segmentation, which is done by three classifiers: ANN, CNN, RF trained on Gabor filter and the tumor segmentation is done by the human visual system (HVS). For pixel-wise segmentation, reliable and accurate ML techniques were used. For the liver segmentation, the classification accuracy was 99.55, 97.88 and 98.13% for RF, CNN and ANN, respectively. From the extracted image of liver, the classification accuracy for tumor was 99.52, 98.07 and 98.45% for RF, CNN and ANN, respectively.

Keywords: Random forest, Convolutional neural network, Artificial neural network, Liver tumor, Segmentation, Gabor filter.

Introduction

In this world, cancer is the second factor of death. In 2015, The World Health Organization (WHO) reports that 788000 died due to liver cancer over 8.8 million deaths. The higher rate of liver cancer cases was found in Southeast Asia and Sub-Saharan Africa, which account more than 600000 fatalities annually. Most of liver cancers can be primary or secondary or liver metastases. The most prevalent main form of liver cancer is hepatocellular carcinoma (HCC). This paper extracts the pixel level features using a set of Gabor filters. The liver is then extracted from an abdominal CT image using liver segmentation, which is done by three classifiers: ANN, CNN, RF trained on Gabor filter and the tumor segmentation is done by the human visual system (HVS), for pixel-wise segmentation reliable and accurate ML techniques were used. A strategy is founded on the training and testing of several labels for the liver and tumor taken from medical images that skilled radiologists and doctors initially segmented. Creating software or a computer-assisted system will allow you to combine these thoroughly tried and confirmed techniques (Bevilacqua V, *et al.*, 2017). Therefore, developing a liver and tumor segmentation algorithm that is accurate and effective without the assistance of a specialist can save many lives.

[1]Department of Electronics and Communication Engineering, Sona College of Technology, Salem, Tamil Nadu, India

[2]Department of Electronics and Communication Engineering, B. S. Abdur Rahman Crescent Institute of Science and Technology, Vandalur, Chennai, Tamil Nadu, India

[3]Department of Electrical and Electronics Engineering, Meenakshi sundararajan Engineering College, Chennai, Tamil Nadu, India

[4]Electronics and Communication Engineering, Kongunadu College of Engineering and Technology, Trichy, Tamil Nadu, India

***Corresponding Author:** N. Sasirekha, Department of Electronics and Communication Engineering, Sona College of Technology, Salem, Tamil Nadu, India, E-Mail: sasikrishni@gmail.com

How to cite this article: Sasirekha, N., Anitha, R., Vanathi, T., Balakrishnan, U. (2023). Automatic liver tumor segmentation from CT images using random forest algorithm. The Scientific Temper, **14**(3): 696-702.

Doi: 10.58414/SCIENTIFICTEMPER.2023.14.3.19

Source of support: Nil

Conflict of interest: None.

Literature Survey

Numerous studies have been conducted to segment the liver and its tumors using manual, auto and semi-auto segmentation techniques. In contrast, the manual segmentation technique concentrates on various sectors, hemi-liver regions or blood vessels to segment the liver. The auto and semi-auto segmentation techniques on various computer-based algorithms to allow the tumors or the liver segmentation from the CT images with varying degrees of number of user interaction. To distinguish the

Received: 10/07/2023 **Accepted:** 17/08/2023 **Published** : 25/09/2023

liver or a tumor from medical photographs, whether using a manual segmentation technique (full hand) or a semi-automatic segmentation technique, always requires the active engagement of an expert of physician. The sections that follow give an overview of the research on tumor and liver segmentation that has been done in the field. By using the procedure of liver segmentation, a medical image is divided into non-liver parenchyma and liver parenchyma (Ronneberger O *et al.,* 2015). There are numerous techniques for segmenting the liver, including active contour, CNN and ANN clustering, deformable model, level set, graph cuts and thresholding. A lot of connected networks have built recently, and while they seem favorable, they are expensive to compute because they need a lot of training data and fast processors. By studying the region's homogeneity feature, an adaptive region expanding technique to autonomously for liver segmentation. This technique under segments when the target is inhomogeneous since it depends on the homogeneity criteria of the tissue.

The procedure of separating tumor cells from liver cells is known as tumor segmentation. For any surgical procedure, tumor segmentation is crucial. For a more effective treatment strategy at different stages of liver cancer, accurate and specific knowledge of the location and shape of the tumor is very important. This enables monitoring the progress of the therapy over time.

Proposed System

We offer two reliable and well-liked supervised neural network techniques, random forest algorithm (RF) as shown in Figure 1 and support vector machine (SVM), which are employed as classifiers to segment liver and tumors. Convolutional neural network (CNN) is another method of classifier used for separating hyperplane. CNN can avoid the issue by using hyperplane. The segmentation of the liver and tumor has been approached in our thesis as a binary classification issue (Ronneberger O *et al.,* 2018). The CNN classifiers to determine whether each point during liver or lesion segmentation is a liver or a tumor cell or not. The CNN ideal hyperplane was used to estimate the distance between the two categories of cells, such as segmentation of liver and tumor (E. Vorontsov *et al.,* 2018). The following sections cover the specifics of each method and how it was used to segment the liver and tumors.

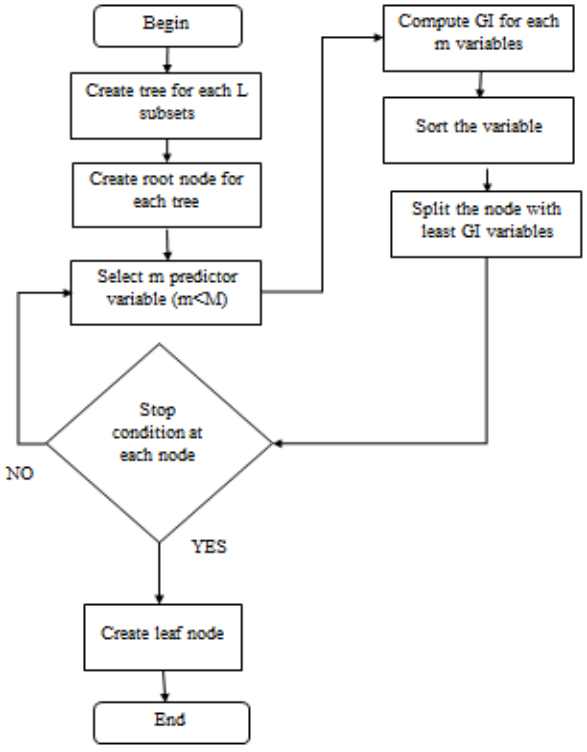

Figure 1: Random forest algorithm

Pre-processing of CT image

Picture pre-processing is a crucial stage in CT image survey, including noise reduction, augmentation, normalization and standardization. There are two types of domains like spectral and spatial domain were used to remove noise from the scanned CT images (P. Campadelli *et al.,* 2007). While adaptive mean filtering makes use of local image statistics to recognize and maintain edges and features, mean filtering blurs and smoothes the image as shown in Figures 2 and 3. When the function of probability density function has a

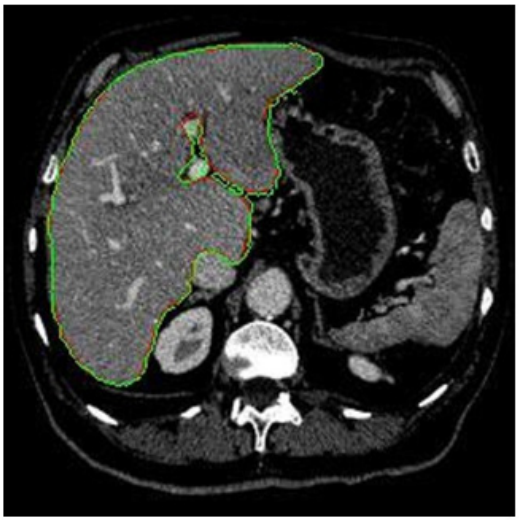

Figure 2: Liver segmentation using random forest

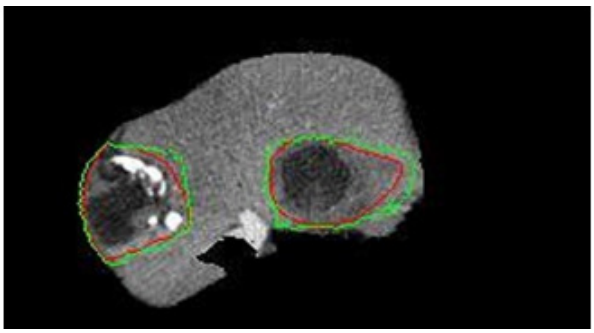

Figure 3: Tumor segmentation using random forest

large tail, order-statistic filters are employed to decrease noise (H. Hwang *et al.,* 1995). A multi-scale transform called a curvelet has frame elements that are indexed by scale and position parameters. Geometric filtering eliminates noise while maintaining crucial information (Nanda N *et al.,* 2019).

These segmented CT pictures are crucial for planning surgery, identifying the tumor's location, and separating tissues from neighboring unnecessary organs (I. Pitas *et al.,* 1992). Some types of spatial domain approaches are mean filtering, nonlinear diffusion, geometric, adaptive mean and maximum a posteriori filtering, etc.

CT scan liver images enhancement with Gabor feature extraction

Gabor filter is used to improve and extract the features of the scanned CT images of the liver. The augmentation is done by both HU and HE. These Hounsfield units are transformed into greyscale image by HU windowing and the image is displayed by making the best use of the available grayscale (A. Goshtasby *et al.,* 2008). An array of Gabor filters, for the

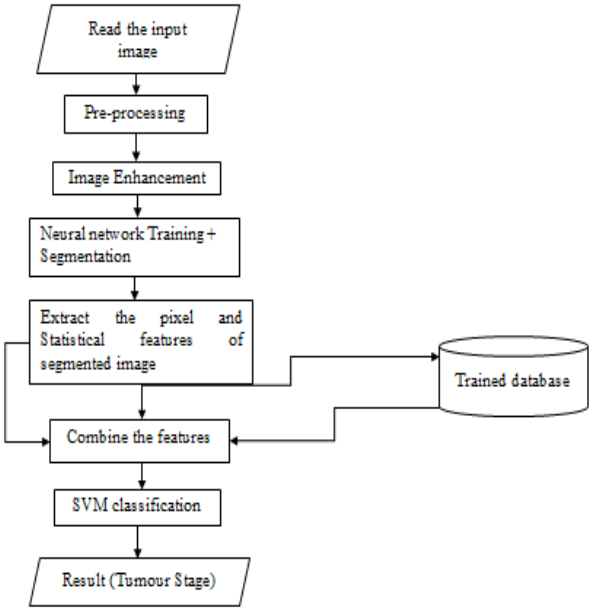

Figure 4: Flowchart of Gabor feature dataset

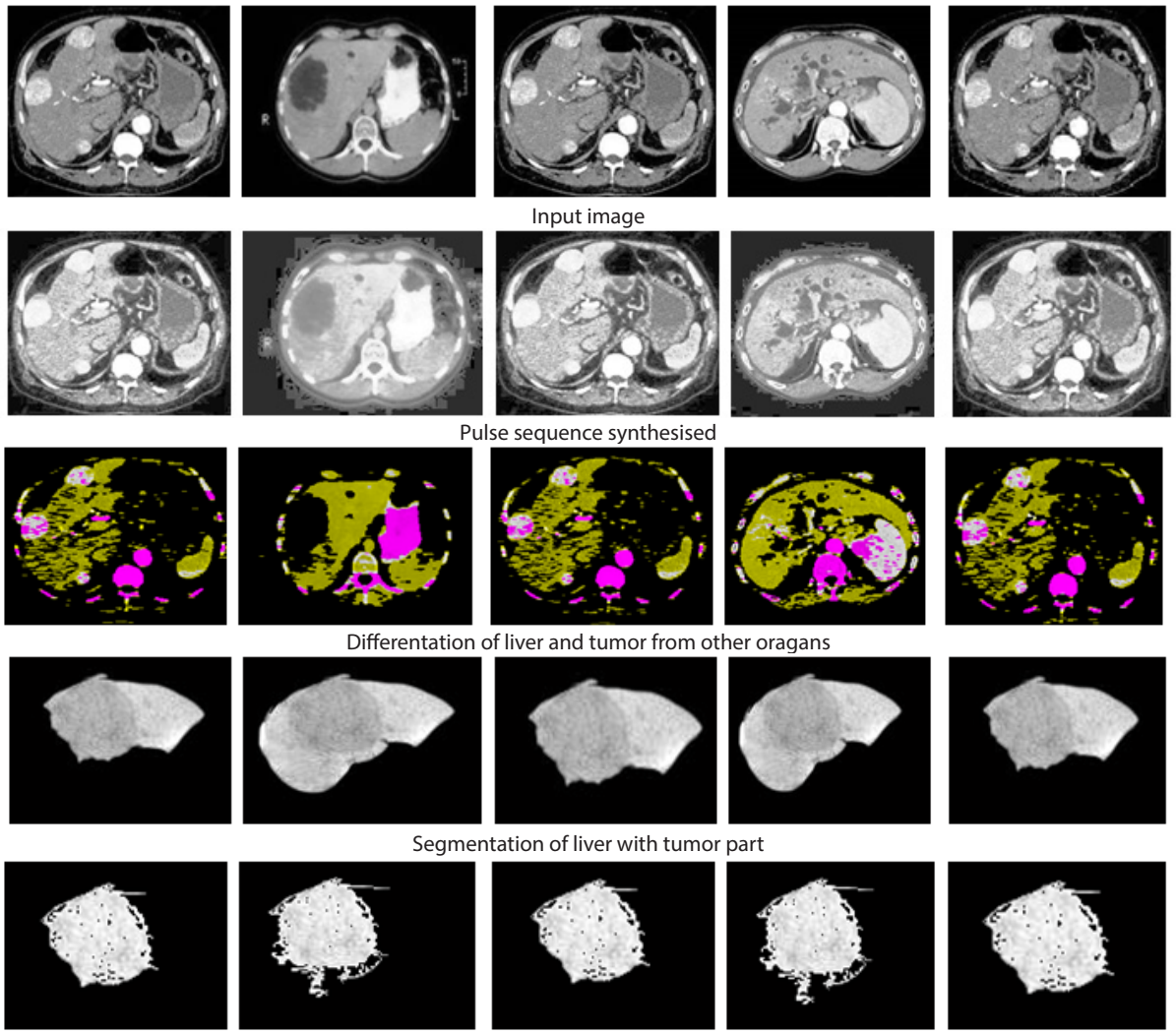

Figure 5: Liver with tumor models

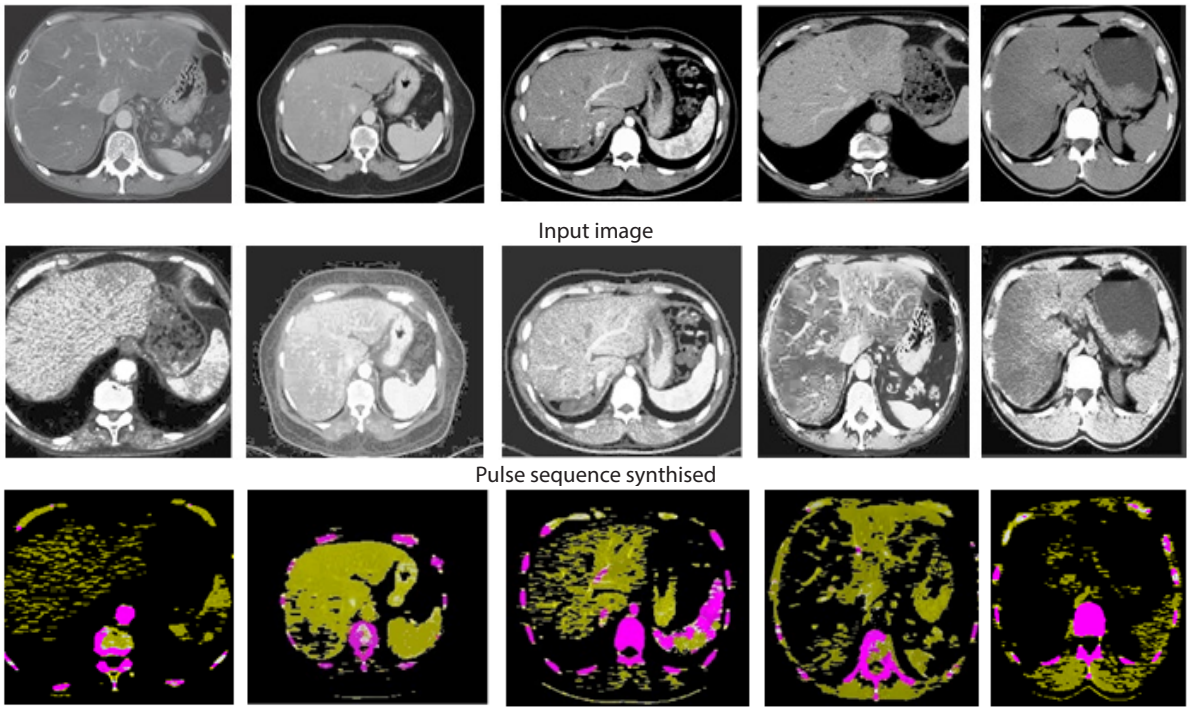

Figure 6: Liver with non-tumor models

texture analysis band-pass filter is used, were utilized to extract the texture information. This filter's degree of scale, rotation, and translation invariance, as well as its best-in-class localization capabilities in spatial domains and frequency, are its benefits (C. Rekeczky *et al.,* 1998).

Hounsfield windowing

Hounsfield windowing removes unnecessary parts or objects from medical images (R. Lamba *et al.,* 2014). HU maps the radio density volume to 256 different colors of grey to emphasis specific structures. In order to produce the liver's Hounsfield scale, a measured attenuation coefficient is linearly transformed. The HU window is mapped to the range of 0 to 255 to create the greyscale image. The HU values beyond the range of -100 to 400 are mapped to 0 or 255.

Gabor feature extractor

A spatial domain liner filter called the Gabor filter (GF) (A. C. Bovik 1991) is used to extract liver and tumor characteristics from abdominal CT images. A complicated sinusoidal plane that a Gaussian envelope has modified makes up its structure (F. Spoor *et al.,* 2000). Given that Gabor wavelets are directly related to the Gabor filter. The input signal is convolved with a GF of various sizes, producing the Gabor space.

Execution of RF classifier for liver tumor segmentation

The RF binary classifier portioned the abdominal CT scanned images into the liver and tumor layer. The training and testing were done using the Gabor-based feature dataset (L. Zeng *et al.,* 2016). By using the training and testing data, the input abdominal CT image is labeled corresponding to the 26 features of Gabor feature dataset as shown in Figure 4. 80% of the trained, 20% of the tested data were used. The class data of liver and the non-liver were correctly blended by randomly shuffling the training data. The test data set was passed into the RF algorithm to get the predicted values (M. Clark *et al.,* 1987). The predicted classes were converted into 256 x 256 picture. Extract from this liver image the Gabor features that were described in image processing as shown in Figures 5 and 6. According to the liver and tumor class image which is manually segmented and provided by the radiologist, each feature set was labeled. This process was repeated to get to the predicted class for the tumor. The 256 x 256 segmented tumor image was obtained by resizing the column vector of the predicted class of the Random Forest algorithm (M. R. Turner. 1986).

Experiments and Results

Performance metrics

Performance metrics results are shown in Tables 1 to 4.

Dice similarity coefficient (DSC)

The amount of overlap between two binary masks is measured using DSC. It is the ratio of the size of the segmentation overlap to the combined size of the two objects. From zero (no overlap) to one (perfect overlap), it has a range was mentioned in Tables 3 and 4. (T. Tan 1995).

It represents the segmentation's full effectiveness. Calculating dice requires the following equation.

$$(A, B) = 2\frac{|A \cap B|}{|A|+|B|}$$

Accuracy

Accuracy is measured as the ratio of accurately segmented samples to all samples. Here, one almost perfectly illustrates a successful segmentation. For accuracy calculations, as mentioned in Table 1 and 2, use the following equation.

$$\text{Accuracy} = \frac{TP+TN}{TP+FP+TN+FN}$$

Where TP is a true positive, FP is a false positive, TN is a true negative and FN is a false negative. (Chlebus G *et al.,* 2018).

Volumetric overlapping error (VOE)

VOE stands for volume overlap error between two sets of voxels. VOE's value ranges from 0 to 1. Zero in this case denotes flawless segmentation. The VOE is determined using the equation below.

$$V(A, B) = 1 - \frac{2|A \cap B|}{|A|+|B|}$$

Average symmetric surface distance (ASD)

To compare the differences between two outlines, ASD is utilized. For the projected segmentation, the collection of surface voxels that is S (P) is used. For the segmentation which is ground truth or reference the set of surface voxels that is S (G) is used (T. G. Dietterich 2000) The distance between the voxel contour of automated and the voxel contour of reference segmentation is called as the Euclidean distance or the average of the shortest distance, which is determined as ASD (J. R. Quinlan 1986).

Simulation Results and Comparison for RF, CNN and ANN

As a binary classifier, RF, CNN, and ANN are created in this thesis. The most popular and significant metrics for statistically assessing the effectiveness of these classifiers are AC, SN, and SP (T. Sørensen 1948). Based on the shared characteristics of the given data set, datasets are split into two classes in a binary classification as shown in Figures 6 and 7. AC determines how accurately a classifier predicts both the negative and the positive classes. (N. Sasirekha *et al.,* 2015).

Results of Proposed Algorithm

The RF, CNN, and ANN are developed as binary classifiers. (L Ramya *et al.,* 2015). The most well-liked and important measures for statistically evaluating these classifiers' efficacy are AC, SN, and SP. Datasets are divided into two classes in a binary classification based on the traits they have in common as shown in Figures 8 and 9. (R Sreelakshmy *et al.,* 2022) In general, SN and SP demonstrate the accuracy of a classifier's positive class prediction, while AC demonstrates the accuracy of its positive and negative class predictions.

Table 1: Sensitivity, specificity and accuracy for liver segmentation

Classifier	*Sensitivity*	*Specificity*	*Accuracy*
RF	0.998	0.994	0.995
CNN	0.997	0.974	0.978
ANN	0.995	0.977	0.981

Table 2: Sensitivity, specificity and accuracy for tumor segmentation

Classifier	*Sensitivity*	*Specificity*	*Accuracy*
RF	0.999	0.993	0.995
CNN	0.999	0.980	0.980
ANN	0.995	0.984	0.984

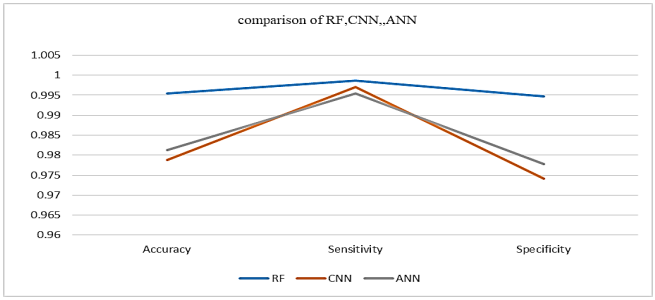

Figure 6: Sensitivity, specificity and accuracy for liver segmentation

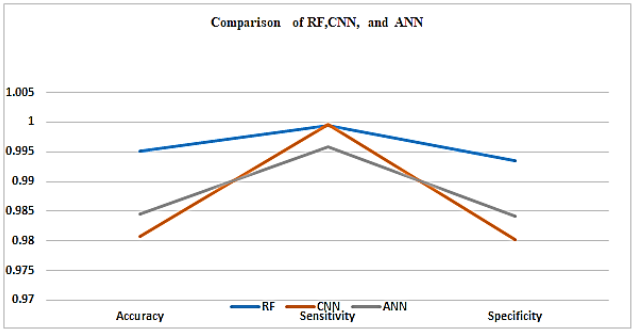

Figure 7: Sensitivity, specificity and accuracy for tumor segmentation

Liver Segmentation

First, in images from an abdominal CT scan, the liver was separated from the other organs. The Gabor characteristics of the CT images trained by the ML algorithms (RF, ANN and

Table 3: Contrast between preferred and other methods for liver segmentation

APPROACH	*ASD (mm)*	*MSD (mm)*	*DSC%*	*VOE%*	*RAVD%*
Method with ANN classifiers	2.98	24.04	97.11	1.89	8.69
Method with CNN classifiers	3.29	25.76	96.79	2.12	10.11
Proposed method with RF classifiers	0.529	3.703	99.03	0.44	1.96
Moghbel et.al	-	-	91.19	5.95	7.49
Zhang et.al	-	24.8	-	5.25	0.73
Kainmiller et.al	1.1	20.9	-	7.0	-3.6

Table 4: Contrast between preferred and other methods for tumor segmentation

APPROACH	*ASD (mm)*	*MSD (mm)*	*DSC%*	*VOE%*	*RAVD%*
Method with ANN classifiers	2.461	13.97	95.65	0.627	-6.25
Method with CNN classifiers	2.419	14.97	96.18	0.613	-4.078
Proposed method with RF classifiers	0.219	1.49	99.43	0.808	0.79
For statistical feature Nan li et al	1.06	8.66	-	26.31	-10.64
Huang et.al	1.06	8.66	-	26.31	-10.64
Cascaded U-net	2.33	46.7	93.1	12.8	-3.3

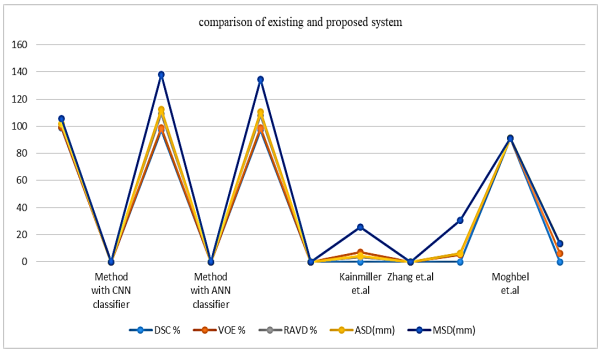

Figure 8: Contrast between preferred and other methods for liver segmentation

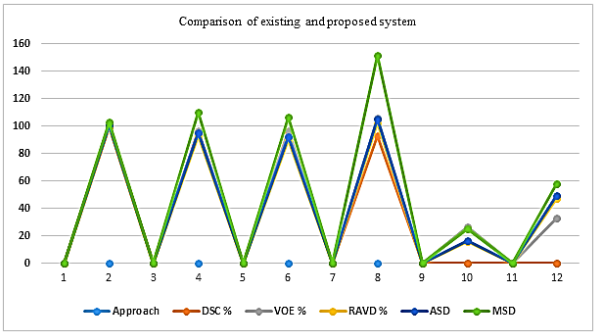

Figure 9: Contrast between preferred and other methods for tumor segmentation

CNN) (L Vanitha *et al.,* 2022). The trained and then tested data were separated with the purpose of segmenting the liver. This step separated the liver from nearby organs and irrelevant tissues.

Tumor Segmentation

The tumor was segmented after obtaining the liver image from step 1 in the previous step. Gabor characteristics were trained by same machine learning algorithms of the segmented image of liver for tumor segmentation (Sasirekha N *et al.,* 2015). In this instance, the positive class is referred to as the tumor cells and the negative class as the liver cells. This step was used to segment the liver tumor.

Conclusion

The liver and the tumor segmentation from the abdominal CT scan images was one of the crucial task for numerous therapeutic applications. The importance of automatic approaches for solving this issue cannot be overstated because they save time, effort, help professionals in their work, and enable early tumor detection and diagnosis. Due to complexity of the liver surface, variations in the size of the liver and tumor across CT imaging slices, and ambiguity in the boundaries of tissues with similar intensities and surrounding objects, segmenting the liver and tumor is a very difficult task. Many studies and efforts have been done in the past to create an automatic and semi-automatic approach for segmenting tumors and the liver. However, only a few techniques segment the images using the liver and tumor. The same method or a single approach yields a better and more precise outcome. The majority of techniques utilised in clinical settings are semi-automatic, requiring some degree of human input during the initial contour definition or parameter modifications, etc. The approaches currently in use were mostly created based on prior research using statistical methodologies. The disadvantages of such strategies include the need for extensive statistical research and the delicate nature of the information-gathering procedure.

More research is necessary to expand this statistical model and the majority of the other approaches mentioned above to other organs or tissues. The new idea behind the suggested broad segmentation technique is training texture features using a neural network approach. With the use of the Gabor feature and three different neural network methods, we applied the theory to the medical area to segment liver and tumors. Several foreseen criteria were employed to demonstrate the suggested method's successful implementation of the individual classifier and segmentation algorithms. The declared method execution offers a view of how this approach might be applied effectively with some tweaks to the same foundations.

This paper major goal was to assess the most widely used and reliable neural network methods (RF, CNN, and ANN) for tumor and liver segmentation with the Gabor feature and contrast the method with other previous work that is stated in Tables 3 and 4. We discovered that the RF classifier with Gabor feature performed better in comparison. The ANN and CNN. While CNN and ANN were outstanding classifiers with classification dice similarity coefficient and accuracy above 95% for both, RF was an excellent classifier. We concluded that the method described here significantly contributes to revealing information regarding the effectiveness, execution, and contrast of three different machine learning algorithms.

Acknowledgment

We are thankful to the management of Sona College of Technology, Salem, India for conducting this collaborative study.

References

A. C. Bovik, (1991). Analysis of multichannel narrow-band filters for image texture segmentation, IEEE Transactions on

signal processing, v. 39, n. 9, p. 2025– 2043.

A. Goshtasby and M. Satter, (2008). An adaptive window mechanism for image smoothing, Computer Vision and Image Understanding, v. 111, n. 2, p. 155–169.

Bevilacqua V, *et al.* (2017). A novel approach for Hepatocellular Carcinoma detection and classification based on triphasic CT Protocol. In: A Novel Approach for Hepatocellular Carcinoma Detection and Classification Based on Triphasic CT Protocol, p. 1856–63.

Chlebus G, Schenk A, Moltz JH, van Ginneken B, Hahn HK, Meine H. (2018). Automatic liver tumor segmentation in CT with fully convolutional neural networks and object-based post processing. Sci Rep, 8:1–7.

C. Rekeczky, T. Roska, and A. Ushida, (1998). CNN-based difference-controlled adaptive nonlinear image filters, International Journal of Circuit Theory and Applications, v. 26, n. 4, p. 375–423.

E. Vorontsov, A. Tang, C. Pal, S. Kadoury, (2018). Liver lesion segmentation informed by joint liver segmentation, in: Proc. - Int. Symp. Biomed. Imaging, vol. 2018–April, IEEE Computer Society, p. 1332–1335,.

F. Spoor, N. Jeffery, and F. Zonneveld, (2000). Imaging skeletal growth and evolution, in Linnean Society Symposium Series, v. 20, p. 123–162.

H. Hwang and R. A. Haddad, (1995). Adaptive median filters: new algorithms and results," IEEE Transactions on image processing, v. 4, n. 4, p. 499–502,.

I. Pitas and A. N. Venetsanopoulos, (1992). Order statistics in digital image processing," Proceedings of the IEEE, v. 80, n. 12, p. 1893–1921.

J. R. Quinlan, (1986). Induction of decision trees," Neural network, v. 1, n. 1, p. 81–106.

L Ramya, N Sasirekha, (2015). A robust segmentation algorithm using morphological operators for detection of tumor in MRI, 2015 International Conference on Innovations in Information, Embedded and Communication Systems (ICIIECS).

L Vanitha, K Jayamani, N Sasirekha, G Sajiv, (2022). Detection and Classification of Breast Cancer from Microscopic Biopsy Images using Modified Neural Network, 2022 International Conference on Automation, Computing and Renewable Systems

L. Zeng, B. Yan, and W. Wang, (2016). Contrast enhancement method based on gray and its distance double-weighting histogram equalization for 3d CT images of pcbs," Mathematical Problems in Engineering, v. 2016.

M. Clark, A. C. Bovik, and W. S. Geisler, (1987). Texture segmentation using gabor modulation/demodulation, Pattern Recognition Letters, v. 6, n. 4, p. 261– 267.

M. R. Turner, (1986). Texture discrimination by gabor functions, Biological cybernetics, v. 55, n. 2, p. 71–82.

Nanda N, Kakkar P, Nagpal S. (2019). Computer-aided segmentation of liver lesions in CT scans using cascaded convolutional neural networks and genetically optimized classifier. Arab J Sci Eng, 44:4049–62.

N. Sasirekha and K. R. Kashwan, (2015). Improved Segmentation of MRI Brain Images by Denoising and Contrast Enhancement, Indian Journal of Science and Technology, v. 8, n. 22, DOI: 10.17485/ijst/2015/v8i22/73050.

P. Campadelli and E. Casiraghi, (2007). Liver segmentation from ct scans: A survey, Applications of Fuzzy Sets Theory, p. 520–528.

R. Lamba, J. P. McGahan, M. T. Corwin, C.-S. Li, T. Tran, J. A. Seibert, and J. M. Boone, (2014). CT hounsfield numbers of soft tissues on unenhanced abdominal CT scans: variability between two different manufacturers mdct scanners, American Journal of Roentgenology, v. 203, n. 5, p. 1013–1020.

Ronneberger O, Fischer P, Brox T. (2015). U-net: Convolutional networks for biomedical image segmentation. In: Proceeding of international conference on medical image computing and computer, p. 234–41.

Ronneberger O, Fischer P, Brox T. (2018). Automatic liver segmentation in abdomen CT images using SLIC and AdaBoost algorithms. In: Proceedings of the 2018 8th international conference on bioscience, biochemistry and bioinformatics. ACM, p. 129-13.

R Sreelakshmy, Anita Titus, N Sasirekha, E Logashanmugam, R Benazir Begam, G Ramkumar, Raja Raju, (2022). An Automated Deep Learning Model for the Cerebellum Segmentation from Fetal Brain Images, v. 2022, Article ID 8342767. https://doi.org/10.1155/2022/8342767.

Sasirekha N, Arun G, (2015). Detection of retinal hemorrhage in color fundus image using splat feature segmentation 2015 International Conference on Innovations in Information, Embedded and Communication Systems (ICIIECS). 10.1109/ICIIECS.2015.7192928.

T. G. Dietterich, (2000). "An experimental comparison of three methods for constructing ensembles of decision trees: Bagging, boosting, and randomization," Machine learning, v. 40, n. 2, p. 139–157.

T. Sørensen, (1948). A method of establishing groups of equal amplitude in plant sociology based on similarity of species and its application to analyses of the vegetation on danish commons, Biol. Skr., v. 5, p. 1–34.

T. Tan, (1995). Texture edge detection by modelling visual cortical channels, Pattern Recognition, v. 28, n. 9, p. 1283–1298.